Using functionalized asphaltenes as effective adsorbents for the removal of chromium and lead metal ions from aqueous solution

Mohammad Nahid Siddiqui [a,*], Shamsh Pervez [b,**], Indrapal Karbhal [b], Princy Dugga [b], Saravanan Rajendran [c], Yasmeen Fatima Pervez [d]

[a] Department of Chemistry and IRC for Membranes and Water Security, King Fahd University of Petroleum & Minerals, Dhahran, 31261, Saudi Arabia
[b] School of Studies in Chemistry, Pt. Ravishankar Shukla University, Raipur, 492010, Chhattisgarh, India
[c] Laboratorio de Investigaciones Ambientales Zonas Áridas, Departamento de Ingeniería Mecánica, Facultad de Ingeniería, Universidad de Tarapacá, Avda. General Velásquez, 1775, Arica, Chile
[d] Department of Chemistry, Government Elvaya College, DOndi-Lohara, Balod, CG, India

ARTICLE INFO

ABSTRACT

For the first time, functionalized asphaltene has been designed, synthesized, and used for the removal of heavy metals from the water. Asphaltene was separated from the crude oil with the addition of n-alkanes. Asphaltene having a complex chemical structure including multilayered and clustered aromatic fused rings bearing aliphatic chains. Asphaltene also contains heteroatoms like N, S, and O atoms along with Ni and V as prominent trace metals. On functionalization of asphaltene with nitric acid, the aliphatic chains and some of the naphthenic rings broke down and developed –COOH, –C═O, C–O, and other oxygen functional groups which are playing key roles as surface-active agents in the removal of the heavy metals via chemisorption. The study was conducted using different parameters such as dose, time, pH, and concentration. The adsorption efficiency for this material at pH 4 is excellent for the removal of chromium and lead. The Langmuir, Freundlich and Temkin adsorption isotherm models as well as Lagergren pseudo second-order kinetic model were investigated. The positive enthalpies ΔHs confirm that the adsorption process is endothermic and the negative free energies ΔGs confirm the spontaneity of the process. The good efficiency of the adsorption implies the efficacy in the removal of the heavy metal ions, as well as the good efficiency in desorption, which implies the excellent recovery of the adsorbent. The effective reusability of this adsorbent makes it applicable for industrial water treatment from contaminants.

1. Introduction

The consumption of crude oil increased dramatically in the last decades. About 70% of the heavy crude oil residue is drilled out and a very small amount is being used without significant process (Speight, 1990).

One of the fractions that are considered as the most troublemaker is the asphaltenes in the refinery and cracking processing of the petroleum, that's due to the precipitation of the asphaltenes can reduce the flow of the oil and also can lead to blockage problems in several types of equipment (Cimino et al., 1995). Moreover, these compounds can form sludges and can deactivate the hydro-desulfurization and hydro-cracking catalysts which lead to a reduction in conversion efficiency for the two processes (Bartholomew, 1994; Miyauchi and de Wind, 1994).

The structure of these compounds was very difficult to study due to their chemical complexity & composition, it was reported that this material is composed of poly-aromatic groups in the center connected with alicyclic and aliphatic groups along with some heteroatoms and some metal ions (Hasan et al., 1988; Shirokoff et al., 1997).

The contamination of water by heavy metal ions is a very serious issue, the source of these metals are different industries such as mining, battery, and other chemical industries. Small concentrations of these heavy metal ions can cause dangerous diseases such as anaemia, cancer, renal and kidney failure, mental retardation, and other serious diseases (Nordberg et al., 2014).

These metal ions are non-biodegradable that's why they need to be removed from the water. There are many methods available for the removal of these materials such as hydroxide or sulfide precipitation, ion

---

exchange, flocculation, membrane separation, and adsorption. Among these methods, adsorption is one of the most promising and effective methods due to its eco-friendly, simple, cost-effectiveness, and applicability for the industry.

Many sorbents are used for the removal of these heavy metals such as activated carbon (Rao et al., 2007), fly ash (Ayala et al., 1998), peat (Ho and McKay, 1999), recycled alum sludge (Chu, 1999), peanut hulls (Brown et al., 2000), resins (Diniz et al., 2002), kaolinite (Arias et al., 2002), zeolite (Biškup and Subotić, 2005), biomaterials, carbon nanomaterial (Ekmekyapar et al., 2006; Li et al., 2004), and multi-walled carbon nanomaterial (Rao et al., 2007) Graphene Oxide (Sahoo and Hota, 2019). But there are several drawbacks for metal oxides due to their poor stability and corrosion. On the other hand, carbon-based materials such as graphene oxide (GO), carbon nanotubes (CNTs), and different forms of carbon have been widely used due to their high surface area, stability, and reusability. Moreover, recently the functionalization of carbon-based materials has attracted great attention due to their strong affinity towards metal ions (Shaikh et al., 2021; Siddiqui, 2017; Siddiqui et al., 2020, 2021; Suliman et al., 2020). Functionalization of carbon-based material can generate high surface active sites such as –OH, –COOH, –C$=$O, -C-O, –NH$_2$, and -S- etc resulting in enhanced hydrophilicity and wettability as well as they play key roles for strong interaction with metal ions by complexation, hard-hard or borderline hard and soft interaction. Although, GO and CNTs have been widely used as an adsorbent but due to their limitations and cost-effectiveness, it is needed to develop low cost, reusable and environmentally friendly materials.

Looking to the current scenario, in this work the asphaltenes have been isolated and functionalized as adsorbents for the removal of water pollutants such as some types of heavy metals ions (Cr and Pb). Hexavalent chromium and lead are known to be mutagenic and carcinogenic in nature (IARC 2012). WHO water quality standards recommend permissible limits of hexavalent Cr (0.05 mg.L^{-1}) and Pb (0.01 mg.L^{-1}) for potable water (WHO, 2017). Many industrial effluents including textile industries, metal finishing, leather tanneries and lead acid batteries are known for higher contents of Cr(VI) and Pb(II) ions and contaminate the adjoining natural water streams and soils (Mahato et al., 2016; Singh et al., 2017). Looking in to the advantages of the functionalized asphaltene, different functional group such as –OH, COOH, –NH$_2$, -S- etc act as chelation centres to bind with metal ions and remove the Cr(VI) and Pb(II) from water via hard-hard or borderline hard and soft interaction (Ravikumar et al., 2016). In cases of most of the environmental samples, Cr(VI) and Pb(II) are found in ionic forms and asphaltene has different functional groups which can bind either with coordinated bond due to presence of lone pair of electron on O, N and C or ion exchange mechanism takes place at certain pH (Xiao and Lin, 2020).

There are several advantages to use functionalized asphaltene such as reusability, low cost, durability, and the presence of surface-active functional groups such as –COOH, –OH, –C$=$O, -C-O, –NH$_2$, and -S- etc show more promising behaviour to adsorb metal ions. Heavy metal ions could interact with the hydrophilic functional group through H-bonding or complexation and electrostatic interaction and can adsorb more metal ions than non-functionalized (Coughlin and Ezra, 1968; McKay et al., 1985; Yang and Xing, 2010).As functionalized asphaltene is metal-free and has high surface-active agents influencing the adsorption performance and can open the new window to develop sustainable material from the waste.

2. Experimental

2.1. Asphaltenes separation

About 7.0 g of Arabian heavy residue was transferred to a beaker and heated with a very small amount of n-heptane. The solution was mixed properly and transferred to 2 L container, then to this solution 700 ml of n-heptane was added. The solution was placed in a mechanical shaker with a water bath. To increase the residue solubility in the heptane, it was heated at 90 $^{\circ}$C for 2 h with continuous stirring. Then the solution was covered using aluminium foil and was stand for cooling overnight. The gradual cooling helps to produce efficient precipitation of asphaltenes. After that, the solution was filtered with 0.8 μm pore size filter paper. The residue part was extracted by soxhlet using toluene as extracting solvent, and the extract was filtered with the same microfilter paper. After the evaporation of the extract, the asphaltenes were collected in a beaker. Then it was washed many times with a small amount of n-heptane. Finally, the solid asphaltene was dried at 105 $^{\circ}$C for 2 h.

2.1.1. Functionalization of asphaltenes

About 10 g of the asphaltenes were dispersed in nitric acid (70%) and the solution was sonicated for 60 min. The mixture was refluxed for 6 h. Then the mixture was cooled down. The functionalized asphaltenes were washed with water many times until the deionized water became clear, then the asphaltenes were dried for 24 h in an oven at 100 $^{\circ}$C and were pulverized in a ball mill.

2.2. Sample characterization

The functionalized asphaltenes were characterized using scanning electron microscopy (SEM) and Fourier transform infrared spectroscopy (FTIR). FESEM/FIB/GIS (Tescan Lyra-3) was used for the morphological studies of the material operated at 20.0 kV. Nicolet 6700 FT-IR spectrometer was used in the range 400–4000 cm^{-1} for the FT-IR spectral measurements of the material. The Brunauer–Emmett–Teller (BET) analysis was performed using a micromeritics (Tristar II PLUS) instrument under the continuous adsorption conditions to determine the surface area.

2.3. Adsorption experiments

The adsorption properties of the adsorbent for Cr and Pb ions were determined by spectrophotometric method; the procedure for heavy metal ions adsorption was as follows: A mixture of adsorbent (200 mg) in 25 ml of 50 mg/L heavy metals ions solution was stirred using a temperature-controlled shaker-bath at various pH for overnight. pH was adjusted using both 0.1M and 1.0M nitric acid and 0.1M and 1M sodium hydroxide solutions; at pH 4 the adsorption was relatively higher than neutral pH. The adsorbent was filtered and the filtrate is then analyzed by an AAS spectrophotometer to find out the remaining heavy metals ion concentration.

The capacity of adsorption (q_{ion}) was calculated by Eq. (1):

$$q_{ions} = \frac{(C_i - C_e)\,V}{W}\ mmol\Big/g \tag{1}$$

Where C_i and C_e are the initial and equilibrium concentrations of heavy metals ion respectively, W is the weight of the adsorbent in g and V is the volume of the solution in a milliliter (Sahoo et al., 2019).

Adsorption kinetic studies were carried out by stirring 25 ml of 50 mg/L solution in a preferred pH buffer with the adsorbent (200 mg) at different temperatures and determining the heavy metals ion concentrations by taking a small amount of filtered aliquots at various time intervals. Adsorption isotherms were constructed by determining the adsorption capacities of the adsorbent at different heavy metals ion Concentration ranging from 10 mg/L to 100 mg/L at ambient temperature. Experiments were carried out at different temperatures, thermodynamic parameters such as a change in enthalpy ΔH, change in free energy ΔG, and change in entropy ΔS were calculated.
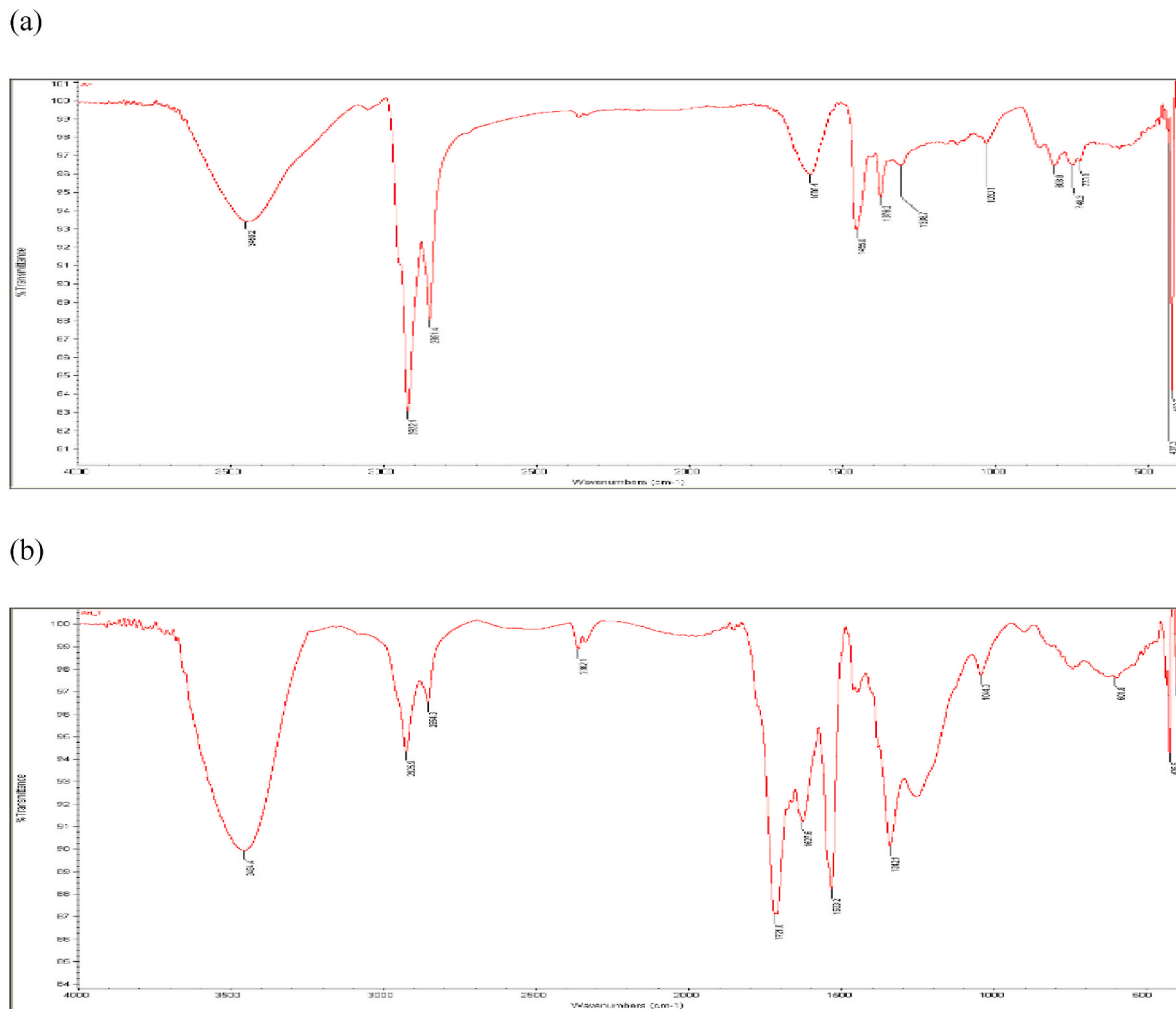
(a)

(b)

Fig. 1. (a) IR spectra of virgin asphaltenes (b) IR spectra of asphaltenes after functionalization.
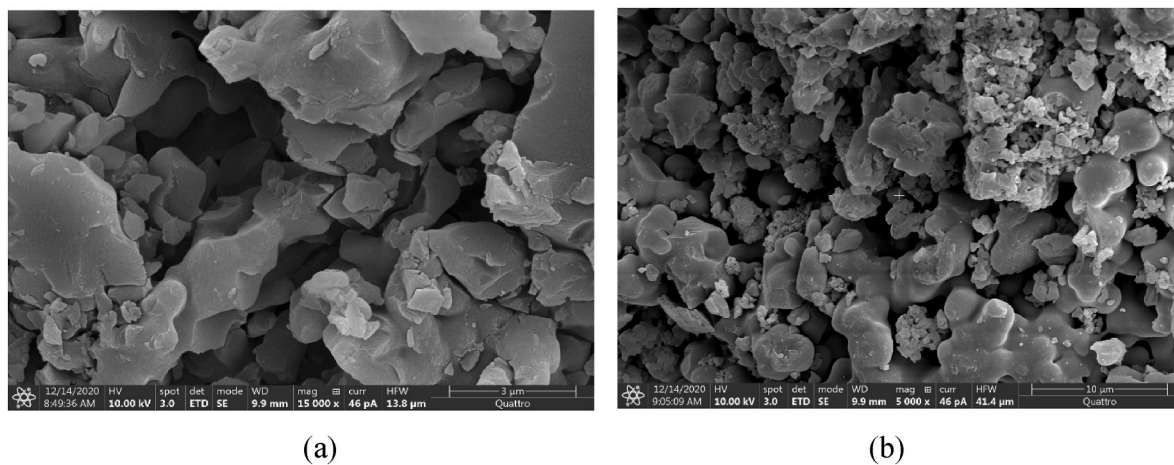

Fig. 2. (a) SEM of AH virgin asphaltenes (b) SEM of AH functionalized asphaltenes.

3. Results and discussion

3.1. Functionalized asphaltenes characterization

The functionalized asphaltenes were characterized using different techniques: SEM, FT-IR, Elemental analysis, and EDX.

Fig. 1 represents the IR spectra of AH asphaltene and functionalized asphaltene. The presence of a broad peak at 3450 cm^{-1} is due to the –OH stretching frequency in both samples. After functionalization, the peak appeared at 1720 cm^{-1}, which confirms the presence of the carbonyl (C=O) group compared to the non-functionalized. Moreover, there are other peaks such as at 2925 cm^{-1} and 2854 cm^{-1} are due to the –NH

Table 1
Elemental analysis (%).

Sample	C	H	N	S	O (by difference)
AH	81.28	7.44	1.19	7.17	2.92
AH-F	57.08	4.13	5.31	5.65	27.83

stretching vibration of the amine group. 1627 cm^{-1} C=C stretching of the aromatic ring, 1533 cm^{-1} is due to NH$_2$ bending, 1455 cm^{-1} is due to C–OH, 1376 cm^{-1} and 1342 cm^{-1} are due to pyridinic ring stretching, 1044 cm^{-1} C–O and stretching vibration and bending vibration of secondary amine, 748 cm^{-1} is due to C–S stretching frequency (Du et al., 2020; Pooja et al., 2017; Sahoo and Hota, 2019) All the data confirm the presence of functional groups in asphaltene which significantly play a key role in the formation of the chelate ring or complex with the metals.

Fig. 2 (a) shows the SEM image of AH virgin asphaltenes and Fig. 2 (b) shows the functionalized asphaltenes. SEM images clearly show the morphological difference between both images.

After functionalization of asphaltene, it became spongy because of the gaining of the extra-functional groups like –OH and –COOH etc.

The type of porosity and the surface area of the virgin asphaltene and funtionalized asphaltene were obtained by the nitrogen adsorption isotherm (BET). The surface area of the virgin asphaltene was found to be 5.4144 m^2/g. However, the functionalized asphaltene has a significantly lower a surface area of 3.8268 m^2/g. This is a substantial drop in the surface area of functionalized asphaltene is due to the development

of oxygen moieties on the surface of virgin asphaltene after functionalization. Similarly, adsorption average pore width was found to be 64.4673 Å for virgin asphaltene and 52.8895 Å for functionalized asphaltene. The higher values of surface area and average pore width in asphaltene are due to the development of several oxygen containing functional and chemical groups on functionalized asphaltene.

Table 1 shows the elemental analysis of asphaltenes and functionalized asphaltenes, this clearly shows the gaining of extra oxygen after functionalization, which has increased from 2.92% to 27.83%. This indicates the very good functionalization of the asphaltenes, and SEM image also reveals the functionalization of asphaltene. Variation in the concentrations (%) of major constituent elements (C, H, N, S) of functionalized asphaltene (carbon C-81.28 to 57.08, H-7.44 to 4.13, N- 1.19 to 5.31 and S- 7.17 to 5.65%) indicates the gaining of extra elements after functionalization These functional groups act as chelating agents and play a key role to bind the metal ions via complexation.

3.2. Adsorption properties of the adsorbent

The adsorbent showed high ion exchange capacity (IEC), and excellent adsorption ability for heavy metal ions due to the presence of different kinds of functional groups available such as –OH, COOH, –C=O, -C-O, –NH$_2$, and -S- etc which are responsible for ion-exchange and complex formation. Because of these functional groups, functionalized asphaltenes show promising adsorbent properties.
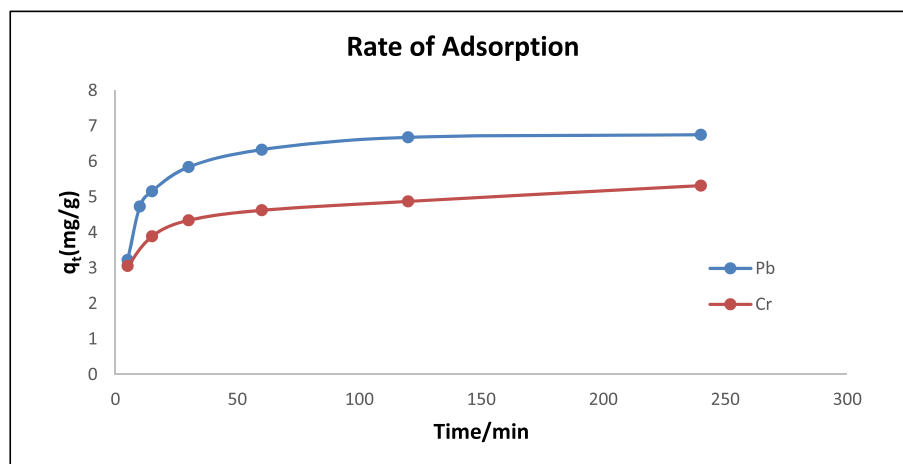

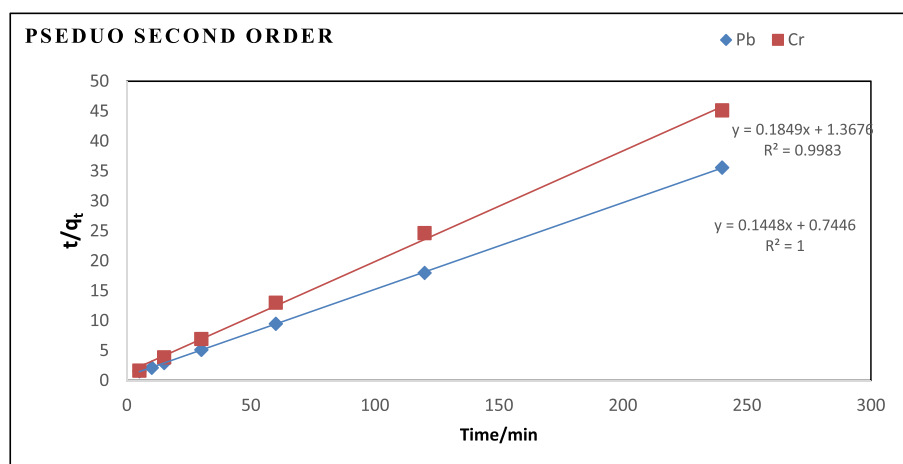**Fig. 3.** Adsorption curves with the time of 25 ppm for Cr & Pb solution at their optimum pH.

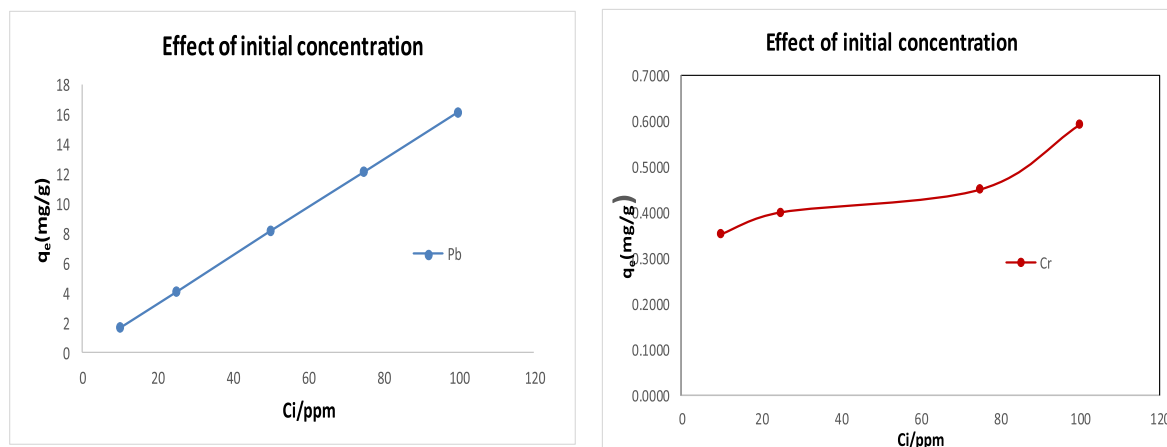**Fig. 4.** Adsorption pseudo second order model for Cr and Pb at 295 K.

Fig. 5. The initial Concentration effect on the removal of heavy metal ions for Pb and Cr for 24 h at 25 0C.

3.3. Adsorption kinetics

A plot of adsorption capacity versus time determines the adsorption rate in the below Fig. 3. It has been found that the adsorption equilibrium for Cr and Pb ions by adsorbent reached about 1.0 h. Lagergren's adsorption kinetic model has been reported as an optimum method to study the properties of adsorption. The kinetic orders were expressed by the equations below (first and second-order models respectively).

$$\log (q_e - q_t) = \log q_e - \frac{k_1 t}{2.303} \qquad (2)$$

$$\frac{t}{q_t} = \frac{1}{k_2 q_e^2} + \frac{t}{q_e} \qquad (3)$$

Where k_1 is the first-order constant and k_2 is the second-order rate constant; q_t and q_e are the capacities of the adsorption for the adsorbent at time t and equilibrium. Although Cr and Pb both gave regression values (R^2) above 0.9 for the pseudo-first-order Lagergren kinetic model. In Fig. 4 linear plot between t/qt and time indicates that Cr and Pb were best fitted for the second-order model and hence more appropriate to explain the adsorption kinetics of both the elements (Fan et al., 2020).

3.4. Initial concentration effect on the removal of Cr and Pb

The adsorption capacity of adsorbent with change in initial concentrations of Cr and Pb metal ions is depicted in Fig. 5. The effect of concentrations of Cr and Pb were observed at the range of 10–100 ppm and all other parameters were kept constant. The adsorption capacity of both Cr and Pb metal ions has shown a significant increase with increasing initial metal ion concentrations. This may probably be due to the driving force provided by the higher initial concentration to

overcome mass transfer barriers between all the molecules of solid and liquid phases which enables the attraction of metal ions from solution onto the surface of functionalized asphaltenes (Gupta et al., 2012).

The Langmuir isotherm is based on the assumptions that on the structurally homogeneous adsorbent, all adsorption sites are energetically equivalent and identical as well as the intermolecular force decreases rapidly with distance. So it follows the mechanism of adsorption of a monolayer on the adsorbent surface. The Langmuir Constants and adsorption capacities can easily be calculated by linearized Langmuir isotherm equation (5) as follows

$$\frac{C_e}{q_e} = \frac{C_e}{Q_m} - \frac{1}{Q_m b} \qquad (4)$$

Where q_e is millimoles of metal adsorbed per gram of the adsorbent; C_e is the metal residual Concentration in solution at equilibrium, Q_m is the maximum specific uptake corresponding to the site saturation and b is the ratio of adsorption and desorption rates, the Langmuir constant (Cabeza et al., 2002). Fig. 6 represents the plot of C_e/q_e versus C_e. On the other hand, the Freundlich isotherm model describes heterogeneous adsorption systems with uniform energy (Fig. 7); the model was expressed by the below equation:

$$Q_e = k_f C_e^{1/n} \qquad (5)$$

$$\log q_e = \log k_f + \frac{1}{n} \log C_e \qquad (6)$$

Where q_e the concentration at the equilibrium of the heavy metal ions on the adsorbent and C_e on the sample solution; the constants k_f and n, can be calculated from the slope and intercept.

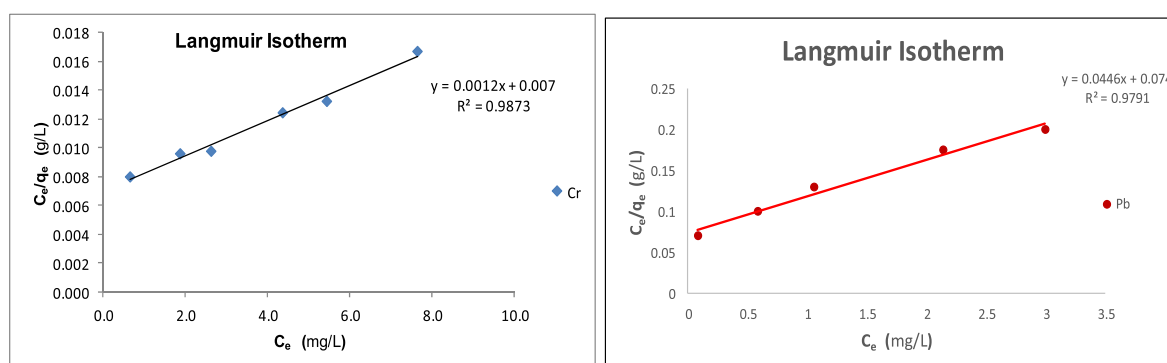The Temkin isotherm equation suggests that owing to adsorbent-

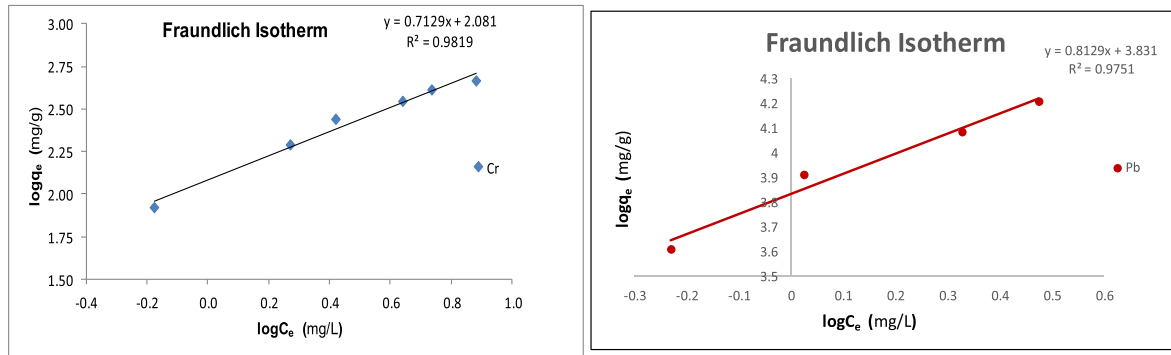**Fig. 6.** Adsorption Langmuir isotherm of Cr and Pb on adsorbent.

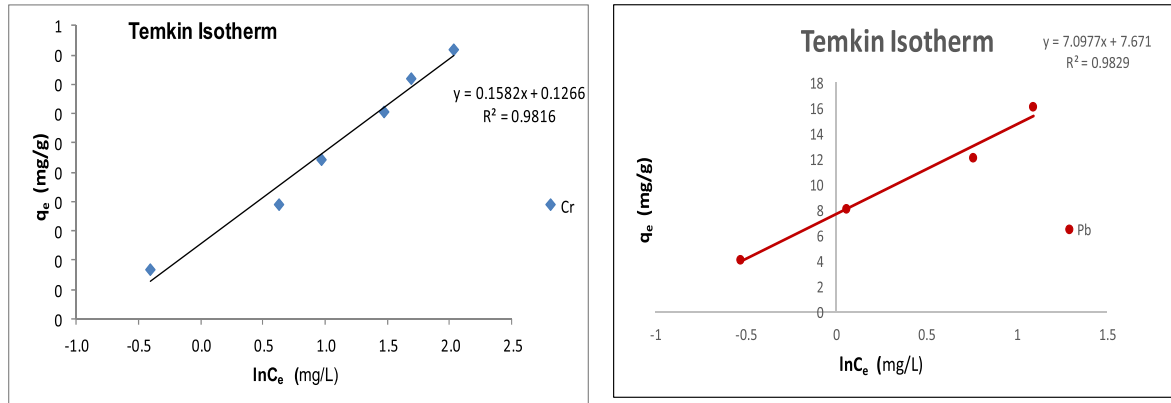**Fig. 7.** Adsorption Freundlich isotherm of Cr and Pb on adsorbent.

Fig. 8. Adsorption Temkin isotherm of Cr and Pb on the adsorbent.

Table 2
Langmuir Freundlich and Temkin isotherm model Constants for Cr and Pb removal.

a)Langmuir isotherm model				
Entry No	Heavy metals ion	Q_m (mmol g^{-1})	b (dm^3 mmol^{-1})	R^2
1	Cr	833.3	0.171	0.987
2	Pb	22.42	0.599	0.980

b)Freundlich isotherm model				
Entry No	Heavy metal ions	n	k_f	R^2
1	Cr	1.402	0.008	0.982
2	Pb	1.230	0.0001	0.975

c)Temkin-isotherm model				
Entry No	Heavy metal ions	B	A	R^2
1	Cr	0.158	2.230	0.982
2	Pb	7.100	2.945	0.983

Table 3
The RL values based on the Langmuir isotherm model.

C_i (mg dm^{-3})	R_L value	
	Cr	Pb
10	0.370	0.143
25	0.190	0.063
50	0.105	0.032
75	0.072	0.022
100	0.055	0.016

Table 2 shows the Langmuir Freundlich and Temkin isotherm model Constants for Cr and Pb removal.

From the figures above we can say that the adsorption of the heavy metal ions on asphaltenes surface could be homogeneous or monolayer because the adsorption obeyed the three above isotherms.

The affinity of the adsorption of the heavy metal ions on the adsorbent surface can be described by the separation factor (R_L) in the Langmuir isotherm is given in eq (9):

$$R_L = \frac{1}{(1 + bC_0)} \tag{9}$$

Where C_o is the initial heavy metals ion concentration and *b* is the Langmuir equilibrium constant. When the value of (R_L) falls between 0 and 1 it indicates the favorability of the adsorption on the adsorbent surface, as its clear in the below Table 3 the value falls in the range, and that means good adsorption favorability for the heavy metal ions on the adsorbent surface.

adsorbate interactions, the heat of adsorption of molecules in layer decreases linearly with Coverage, and the adsorption is characterized by a uniform distribution of the binding energies. The Temkin isotherm can be expressed by the following equation:

$$q_e = \frac{RT}{b} \ln(AC_e) \tag{7}$$

and can be linearized as:

$$q_e = B \ln A + B \ln C_e \tag{8}$$

Where *B* Corresponds to the adsorption potential of the adsorbent (KJ/mol), *A* is the Temkin isotherm Constant (L/g). A plot of qe versus lnCe (Fig. 8) is used to calculate the Temkin isotherm Constants A and B.
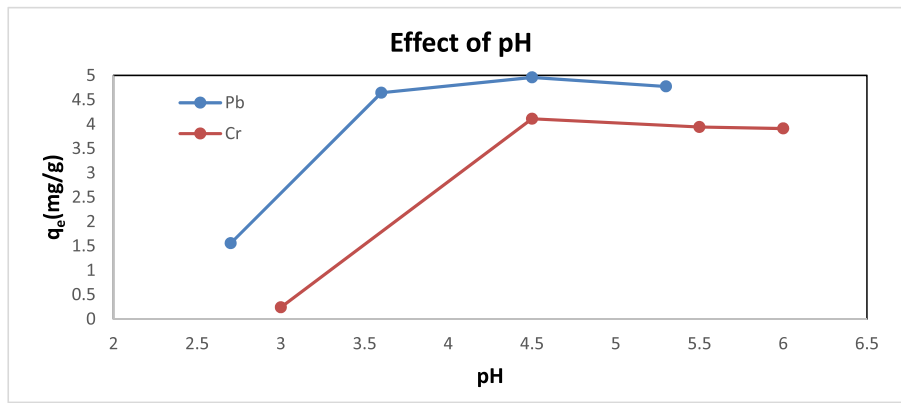
Fig. 9. pH dependence of heavy metal ions uptake by the adsorbent.
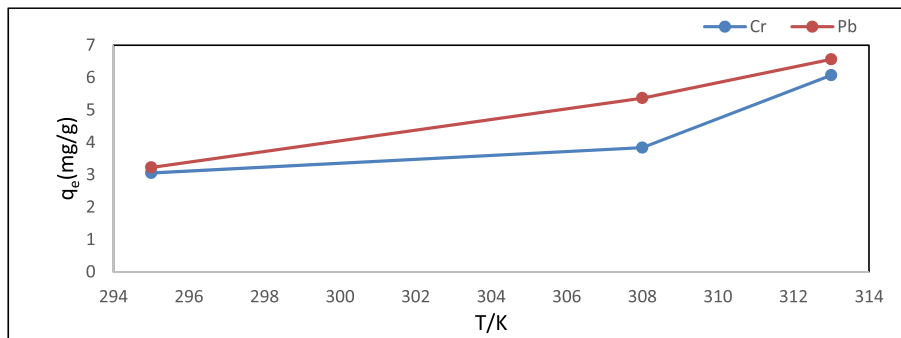

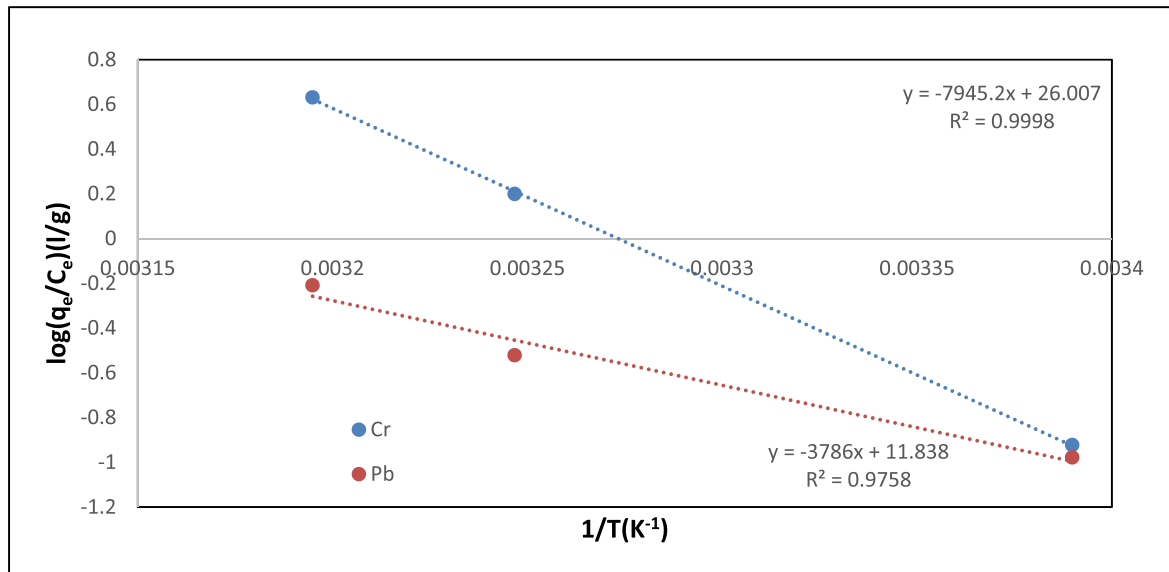**Fig. 10.** Effect of temperature on the adsorption capacity of the adsorbent.

Fig. 11. Vant-Hoff`s plot for adsorption of Pb and Cr on adsorbent.

3.5. pH and temperature effect on the removal

pH is an important parameter that determines the effectiveness of the adsorption process as with the varying pH of the solution, the degree of ionization and surface properties of adsorbent also varies. The experiment demonstrating the effect of pH on the adsorption capacity of Pb and Cr metal ions was carried out at pH ranging between 2.5 – 5 and 3–6 respectively by using acetate buffer. The optimum pH was found to be 4.5 for Cr and Pb. This could be explained that at lower pH, due to

protonation functional groups that are present at the surface are most likely linked with H^+ ions, which makes them inaccessible for metal ions. At moderate pH, functional groups get deprotonated due to which the probability of attachment of metal ions increases, and hence adsorption capacity also increases. At higher pH i.e. above pH 4.5 complexes of soluble hydroxide form which tend to decrease the adsorption capacity of Cr and Pb ions. Fig. 9 indicates pH dependence of heavy metal ions uptake by the adsorbent.

The thermodynamic parameters were obtained from the adsorption

Table 4
Thermodynamic Data for Cr and Pb adsorption.

Heavy metals ion	Temp	ΔG	ΔH	ΔS	R^2
		KJ.mole^{-1}	KJ.mole^{-1}	J.K^{-1}mole^{-1}	
Cr	295	−298.87	−152.07	497.64	0.9998
Pb	295	−139.09	−724.64	225.85	0.9758

The comparative Table S1 and Table S2 have been given in the supporting information for the adsorption efficiency of Cr and Pb respectively and showing very good removal efficiency of functionalized asphaltenes than other adsorbents.

Table 5
The adsorbent regeneration using 0.1M H$_2$SO$_4$ and HCl on Chromium and Lead Adsorbent.

(a) Treatment of 0.1M H$_2$SO$_4$ on Chromium & Lead Adsorbent			
S.No	Sample time	Cr (mg/L)	Pb (mg/L)
1	10min	0.00	3.41
2	30min	0.00	3.21
3	60min	0.00	3.57
4	120min	0.00	4.19
5	24 Hr	0.00	3.98

(a) Treatment of HCl 0.1 M on Chromium & Lead Adsorbent			
S.No	Sample time	Cr (mg/L)	Pb (mg/L)
1	10min	0.00	213.00
2	30min	0.00	214.00
3	60min	0.00	210.00
4	120min	0.00	211.00
5	24 Hr	0.00	219.00

Table 6
The reusability of the adsorbent for a) Cr and b)Pb.

S.No	Sample time	Cr (mg/L)
1.00	15min	19.74
2.00	30min	17.58
3.00	60min	14.04
4.00	120min	8.80
5.00	24 Hr	8.00

S.No	Sample time	Pb (mg/L)
1.00	15min	49.90
2.00	30min	46.17
3.00	60min	45.19
4.00	120min	43.58
5.00	24 Hr	42.52

experiment, and the results were explained in the figure below. As clear in Fig. 10, the removal efficiency increases with the temperature, which means the adsorption is endothermic.

A plot of log (qe/Ce) against 1/T (Fig. 11) using the Vant-Hoff equation the thermodynamic parameters were obtained, and are tabulated in Table 4 (Coşkun et al., 2006; Ramesh et al., 2007). The negative free energies ΔGs confirm the spontaneity of the process.

$$log\left(\frac{q_e}{C_e}\right) = -\frac{\Delta H}{2.303RT} + \frac{\Delta S}{2.303\,R} \tag{10}$$

The negativity of ΔG increases with the temperature that shows that the adsorption is more favorable at higher temperatures. Favorable adsorption at higher temperatures is attributed to the greater swelling of the adsorbent and increased diffusion of heavy metal ions into the adsorbent. The positive enthalpies ΔHs confirm that the adsorption process is endothermic. In addition, it can be found in Table 6 that the ΔS values are positive, suggesting that the randomness increased during adsorption of metal ions because of the release of water molecules from the large hydration shells of the metal ions.

4. Adsorbent regeneration and reuse

The regeneration and the reusability of the adsorbent were investigated for the two contaminants (Table 5(a)(b) and 6(a)(b)), two solutions were used for the regenerate 0.4g of the adsorbent was placed in 30 ml of 0.1M sulfuric acid solution and 0.1M hydrochloric acid and the desorption time was from 10 min to 24 h, as we can see in the table below the Pb ions were almost removed from the adsorbent in hydrochloric solution but it didn't desorb from the adsorbent in sulfuric acid solution, the Cr ions showed good desorption efficiency in both solutions.

The reusability of the adsorbent also was investigated by taking the regenerated adsorbent from the first part washed it with water and dried for overnight then it was placed in a 200 ppm solution of chromium and lead ions, as clear in the below tables the adsorbent was reusable, and the adsorbent showed higher adsorption capacity toward the lead ions.

5. Conclusion

A novel adsorbent from the functionalization of asphaltenes was prepared to form low-cost material with very good yield. The adsorbent was found to have a good removal efficiency for Cr and Pb ions due to the development of functional groups such as –C═O, –COOH, -C-O, and others. These functional groups are responsible for the ion exchange and complexation with the metals. The adsorption process obeyed Langmuir, Freundlich and Temkin isotherm models and, also fitted Lagergren pseudo second-order kinetic model. The positive enthalpies ΔHs confirm that the adsorption process is endothermic, the negative free energies ΔGs confirm the spontaneity of the process. The good efficiency of the adsorption implies the efficacy in the removal of the heavy metal ions, as well as the good efficiency in desorption, which implies the excellent recovery of the adsorbent. The effective reusability of this adsorbent makes it applicable for industrial water treatment from contaminants. As functionalized asphaltene is metal-free as well as has high surface-active agents influencing the adsorption performance of the materials and this process can open a new avenue to develop sustainable material from the waste.

Author contributions

Mohammad Nahid Siddiqui: Conceptualization, Funding acquisition, Writing – original draft preparation, Supervision. Shamsh Pervez: Conceptualization, Writing – original draft preparation, Supervision. Indrapal Karbhal: Writing – review & editing. Princy Dugga: Writing – review & editing, Saravanan Rajendran: Writing – review & editing. Yasmeen Fatima Pervez: Writing – review & editing.

Declaration of competing interest

The authors declare that they have no known competing financial interests or personal relationships that could have appeared to influence the work reported in this paper.

Acknowledgments

Appendix A. Supplementary data

Supplementary data to this article can be found online at https://doi.org/10.1016/j.envres.2021.112361.

References

Arias, M., Barral, M.T., Mejuto, J.C., 2002. Enhancement of copper and cadmium adsorption on kaolin by the presence of humic acids. Chemosphere 48, 1081–1088. https://doi.org/10.1016/S0045-6535(02)00169-8.

Ayala, J., Blanco, F., García, P., Rodriguez, P., Sancho, J., 1998. Asturian fly ash as a heavy metals removal material. Fuel 77, 1147–1154. https://doi.org/10.1016/S0016-2361(98)00027-1.

Bartholomew, C.H., 1994. In: Oballa, M.C., Shih, S.S. (Eds.), Catalytic Hydroprocessing of Petroleum and Distillates. Marcel Decker, New York, p. 42.

Biškup, B., Subotić, B., 2005. Removal of heavy metal ions from solutions using zeolites. III. Influence of sodium ion concentration in the liquid phase on the kinetics of exchange processes between cadmium ions from solution and sodium ions from zeolite A. Separ. Sci. Technol. 39, 925–940. https://doi.org/10.1081/ss-120028454.

Brown, P., Atly Jefcoat, I., Parrish, D., Gill, S., Graham, E., 2000. Evaluation of the adsorptive capacity of peanut hull pellets for heavy metals in solution. Adv. Environ. Res. 4, 19–29. https://doi.org/10.1016/S1093-0191(00)00004-6.

Cabeza, A., Ouyang, X., Sharma, C.V.K., Aranda, M.A.G., Bruque, S., Clearfield, A., 2002. Complexes formed between nitrilotris(methylenephosphonic acid) and M2+ transition metals: isostructural organic-inorganic hybrids. Inorg. Chem. 41, 2325–2333. https://doi.org/10.1021/ic0110373.

Chu, W., 1999. Lead metal removal by recycled alum sludge. Water Res. 33, 3019–3025. https://doi.org/10.1016/S0043-1354(99)00010-X.

Cimino, R., Correra, S., Del Bianco, A., Lockhart, T.P., 1995. Asphaltenes: Fundamentals and applications. Plenum Press, New York, pp. 97–130.

Coşkun, R., Soykan, C., Saçak, M., 2006. Removal of some heavy metal ions from aqueous solution by adsorption using poly(ethylene terephthalate)-g-itaconic acid/acrylamide fiber. React. Funct. Polym. 66, 599–608. https://doi.org/10.1016/j.reactfunctpolym.2005.10.012.

Coughlin, R.W., Ezra, F.S., 1968. Role of surface acidity in the adsorption of organic pollutants on the surface of carbon. Environ. Sci. Technol. 2, 291–297. https://doi.org/10.1021/es60016a002.

Diniz, C.V., Doyle, F.M., Ciminelli, V.S.T., 2002. Effect of pH on the adsorption of selected heavy metal ions from concentrated chloride solutions by the chelating resin Dowex M-4195. Separ. Sci. Technol. 37, 3169–3185. https://doi.org/10.1081/SS-120006155.

Du, L., Gao, P., Meng, Y., Liu, Y., Le, S., Yu, C., et al., 2020. Highly efficient removal of Cr(VI) from aqueous solutions by polypyrrole/monodisperse latex spheres. ACS Omega 5, 6651–6660. https://doi.org/10.1021/acsomega.9b04438.

Ekmekyapar, F., Aslan, A., Bayhan, Y.K., Cakici, A., 2006. Biosorption of copper(II) by nonliving lichen biomass of Cladonia rangiformis hoffm. J. Hazard Mater. 137, 293–298. https://doi.org/10.1016/j.jhazmat.2006.02.003.

Fan, Y., Wang, H., Deng, L., Wang, Y., Kang, D., Li, C., Chen, H., 2020. Enhanced adsorption of Pb(II) by nitrogen and phosphorus co-doped biochar derived from Camellia oleifera shells. Environ. Res. 191, 110030. https://doi.org/10.1016/j.envres.2020.110030.

Gupta, V.K., Ganjali, M.R., Nayak, A., Bhushan, B., Agarwal, S., 2012. Enhanced heavy metals removal and recovery by mesoporous adsorbent prepared from waste rubber tire. Chem. Eng. J. 197, 330–342. https://doi.org/10.1016/j.cej.2012.04.104.

Ho, Y.S., McKay, G., 1999. The sorption of lead(II) ions on peat. Water Res. 33, 578–584. https://doi.org/10.1016/S0043-1354(98)00207-3.

IARC Working Group on the Evaluation of Carcinogenic Risks to Humans, 2012. Chemical agents and related occupations. IARC Monogr. Eval. Carcinog. Risks Hum. 100, 9–562.

Li, Q., Wu, S., Liu, G., Liao, X., Deng, X., Sun, D., Hu, Y., Huang, Y., 2004. Simultaneous biosorption of cadmium (II) and lead (II) ions by pretreated biomass of Phanerochaete chrysosporium. Separ. Purif. Technol. 34, 135–142. https://doi.org/10.1016/S1383-5866(03)00187-4.

Mahato, M.K., Singh, P.K., Tiwari, A.K., Singh, A.K., 2016. Risk assessment due to intake of metals in groundwater of east bokaro coalfield, Jharkhand, India. Expo. Heal. 8, 265–275. https://doi.org/10.1007/s12403-016-0201-2.

McKay, G., Otterburn, M.S., Aga, A.J., 1985. Fuller's earth and fired clay as absorbents for dyestuffs external mass transport processes during adsorption. Water Air Soil Pollut. 24, 307–322.

Miyauchi, Y., de Wind, M., 1994. Hydroprocessing. In: Proceedings of the Akzo Nobel Catalysts Symposium, Amsterdam, The Netherlands, pp. 123–140.

Nordberg, G.F., Fowler, B.A., Nordberg, M., Friberg, L., 2014. Handbook on the Toxicology of Metals. Academic press, New York.

Pooja, D., Saini, S., Thakur, A., Kumar, B., Tyagi, S., Nayak, M.K., 2017. A "Turn-On" thiol functionalized fluorescent carbon quantum dot based chemosensory system for arsenite detection. J. Hazard Mater. 328, 117–126. https://doi.org/10.1016/j.jhazmat.2017.01.015.

Ramesh, A., Hasegawa, H., Maki, T., Ueda, K., 2007. Adsorption of inorganic and organic arsenic from aqueous solutions by polymeric Al/Fe modified montmorillonite. Separ. Purif. Technol. 56, 90–100. https://doi.org/10.1016/j.seppur.2007.01.025.

Rao, G.P., Lu, C., Su, F., 2007. Sorption of divalent metal ions from aqueous solution by carbon nanotubes: a review. Separ. Purif. Technol. 58, 224–231. https://doi.org/10.1016/j.seppur.2006.12.006.

Ravikumar, K.V.G., Kumar, D., Kumar, G., Mrudula, P., Natarajan, C., Mukherjee, A., 2016. Enhanced Cr(VI) removal by nanozerovalent iron-immobilized alginate beads in the presence of a biofilm in a continuous-flow reactor. Ind. Eng. Chem. Res. 55, 5973–5982. https://doi.org/10.1021/acs.iecr.6b01006.

Sahoo, S.K., Hota, G., 2019. Amine-functionalized GO decorated with ZnO-ZnFe2O4 nanomaterials for remediation of Cr(VI) from water. ACS Appl. Nano Mater. 2, 983–996. https://doi.org/10.1021/acsanm.8b02286.

Shaikh, A.R., Chawla, M., Hassan, A.A., Abdulazeez, I., Salawu, O.A., Siddiqui, M.N., Shamsh Pervez, S., Cavallo, L., 2021. Adsorption of industrial dyes on functionalized and nonfunctionalized carbon: A combined molecular dynamics and quantum mechanics study. J. Mol. Liquids 337, 116433. https://doi.org/10.1016/j.molliq.2021.116433.

Shirokoff, J.W., Siddiqui, M.N., Ali, M.F., 1997. Characterization of the structure of Saudi crude asphaltenes by X-ray diffraction. Energy and Fuels 11, 561–564. https://doi.org/10.1021/ef960025c.

Siddiqui, M.N., 2017. Developing an effective adsorbent from asphaltene for the efficient removal of dyes in aqueous solution. Desalin. Water Treat. 67, 371–380. https://doi.org/10.5004/dwt.2017.20450.

Siddiqui, M.N., Ali, I., Asim, M., Chanbasha, B., 2020. Quick removal of nickel metal ions in water using asphalt-based porous carbon. J. Mol. Liquids 308, 113078. https://doi.org/10.1016/j.molliq.2020.113078.

Siddiqui, M.N., Basheer, C., Al-Arfaj, A.A., Kon'kova, T., Ali, I., 2021. Super-fast removal of cobalt metal ions in water using inexpensive mesoporous carbon obtained from industrial waste material. Environ. Technol. Innovat. 21, 101257 https://doi.org/10.1016/j.eti.2020.101257.

Singh, H., Pandey, R., Singh, S.K., Shukla, D.N., 2017. Assessment of heavy metal contamination in the sediment of the River Ghaghara, a major tributary of the River Ganga in Northern India. Appl. Water Sci. 7, 4133–4149. https://doi.org/10.1007/s13201-017-0572-y.

Speight, J.G., 1990. Fuel Science and Technology Handbook. Marcel Dekkar, New York.

Suliman, M.H., Siddiqui, M.N., Chanbasha, B., 2020. Surface functionalization of mesoporous carbon for the enhanced removal of strontium and cesium radionuclides. Coatings 10 (10), 923. https://doi.org/10.3390/coatings10100923.

WHO (World Health Organization), 2017. Guidelines for Drinking-Water Quality: Fourth Edition Incorporating the First Addendum. WHO, Geneva.

Xiao, C., Lin, J., 2020. Efficient removal of Cr(VI) ions by a novel magnetic 4-vinyl pyridine grafted Ni3Si2O5(OH)4multiwalled nanotube. ACS Omega 5, 23099–23110. https://doi.org/10.1021/acsomega.0c02874.

Yang, K., Xing, B., 2010. Adsorption of organic compounds by carbon nanomaterials in aqueous phase: polanyi theory and its application. Chem. Rev. 110, 5989–6008. https://doi.org/10.1021/cr100059s.